Synthetic routes to novel fluorogenic pyronins and silicon analogs with far-red spectral properties and enhanced aqueous stability

Garance Dejouy[a,†], Kevin Renault[a,†], Ibai E. Valverde[a], Anthony Romieu[a,‡]

[a]*Institut de Chimie Moléculaire de l'Université de Bourgogne, UMR 6302, CNRS, Univ. Bourgogne Franche-Comté, 9, Avenue Alain Savary, 21000 Dijon, France*

Abstract

Fluorogenic detection of reactive (bio)analytes is often achieved with "smart" probes, whose activation mechanism causes the release of aniline-based fluorophores. Indeed, the protection-deprotection of their primary amino is the simplest way to induce dramatic and valuable changes in spectral features of the fluorogenic reporter. In this context, and due to their small size and intrinsic hydrophilicity, we focused on pyronin dyes and related heteroatom analogs (*i.e.*, formal derivatives of 3-imino-3*H*-xanthen-6-amine and its silicon analog) for their use as optically tunable aniline-based fluorophores. To overcome some severe limitations associated with the use of such fluorogenic scaffolds (*i.e.*, poor aqueous stability and spectral features only in the green-yellow spectral range), the synthesis of novel unsymmetrical derivatives of (Si)-pyronins bearing a single bulky tertiary aniline (*i.e.*, *N*-methylindoline and julolidine) was explored and presented in this Article. This structural alteration has been found to be beneficial to dramatically lower electrophilicity of the *meso*-position and to reach attractive fluorescence properties within the far-red spectral region.

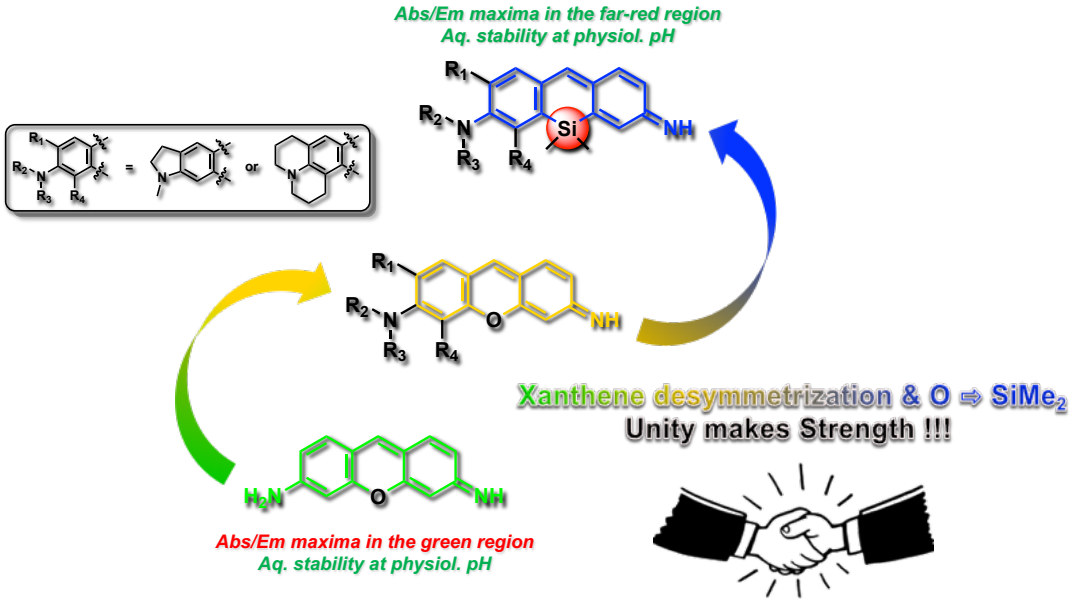

† These authors contributed equally to this work.

‡ Corresponding author. Tel. +33 3-80-39-36-24 ; e-mail anthony.romieu@u-bourgogne.fr

1. Introduction

Among the various types of fluorescent molecules belonging to the xanthene family (*i.e.*, all molecules being derived from the same molecular unit, namely 9*H*-xanthene)[1], pyronin dyes occupy a unique and even paradoxical position compared to other popular subclasses such as fluoresceins [2], rhodamines [3-8], rhodols [9] and rosamines [10]. Indeed, due to their structural simplicity [11], their preparation through formal condensation between one molecule of formaldehyde and two molecules of 3-(dialkylamino)phenols [12,13], was considered shortly thereafter the discovery and synthesis of fluorescein and tetramethylrhodamine by von Bayer (ca. in 1871) and Ceresole (ca. in 1887) respectively [14]. However, for several decades, only the historic symmetrical pyronin dyes (pyronin B and pyronin Y also known as pyronin G, Fig. 1) have been practically used, especially as biological staining agents visualized by fluorescence microscopy [1,15]. In contrast to chemistry of fluoresceins and rhodamines that has been the subject of many spectacular and valuable advances [14], few efforts directed to synthesis, structural and properties optimization of pyronin-based fluorophores have been done until recently [16-19]. The current growing interest for reactivity-based fluorescent probes changes things somewhat. Indeed, the number of chemo/biosensing or bioimaging agents using a pyronin as fluorogenic label, and rationally designed to address specific analytical or biological questions, is constantly rising, leading to new requirements in terms of spectral and physico-chemical properties for the selected photoactive unit [20-33] (Fig. 1). Among the different fluorescent probe design strategies commonly used for selective detection of (bio)analytes through chemical reactions, those based either on (1) protection-deprotection of an amino group (*i.e.*, aniline-based pro-fluorophores) [34-36] or (2) "covalent-assembly" principle [37] are readily implementable to pyronin scaffolds. Some recent examples of the literature illustrate this trend and highlight benefits in terms of sensing performances, that might accrue form it [38-42] (Fig. 1).

In this context, we strongly believe that chemistry of unsymmetrical pyronin structures bearing a primary aniline (*i.e.*, an optically tunable amino group) is worthwhile exploring, both to identify novel fluorogenic scaffolds with valuable properties and to devise novel synthetic routes to high-performance pyronin fluorophores. To the best of our knowledge, only two examples of primary anilines based on pyronin scaffold have already been described in the literature (3-imino-3*H*-xanthen-6-amine and **AR116**, Fig. 1) [40,43]. A one-step synthesis through a conventional acid-catalyzed condensation reaction (*vide supra*) provides after tedious and time-consuming purification procedures these fluorophores in poor to modest

yields even if our group has recently proposed a less straightforward but more effective synthetic approach towards these fluorophores [42].

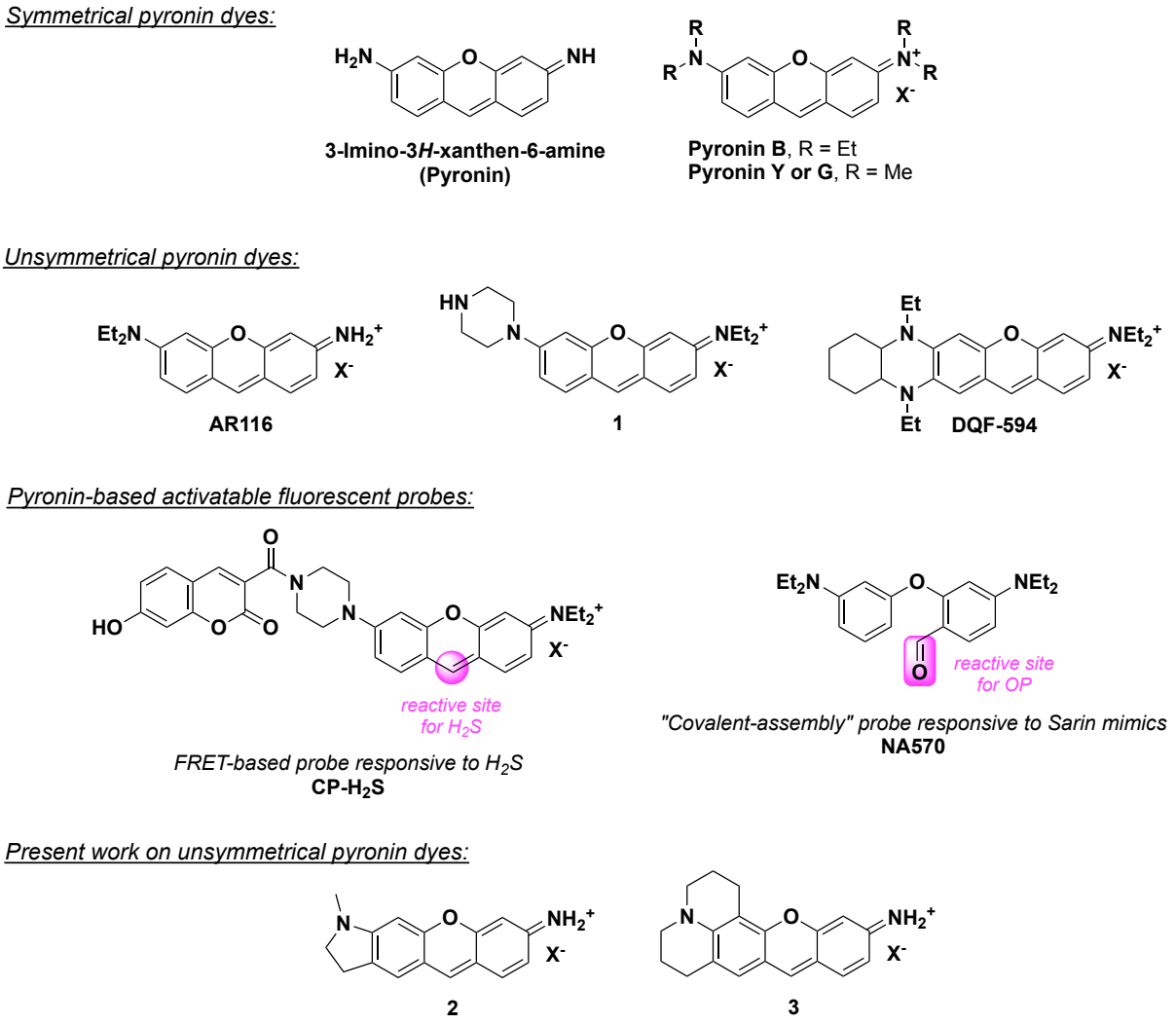

Fig. 1. Structures of the most popular pyronins and unsymmetrical derivatives reported in the literature [24,40,44]; selected examples of reaction-based fluorescent probes based either on FRET mechanism or "covalent-assembly" principle [24,38]; structures of unsymmetrical pyronin dyes studied in the present work (X = Cl^- for **pyronin B** and **Y**, X^- = $CF_3CO_2^-$ for **AR116**, **2** and **3**, for **DQF-594** and **CP-H₂S**, the nature of X^- was not specified by the authors).

Another valuable feature of pyronin scaffold is the facile modulation of its absorption and fluorescence maxima through the formal replacement of intracyclic oxygen atom by a group 14 element (*i.e.*, CMe_2 [45-47], $SiMe_2$ [26,44,48,49], or $GeMe_2$ [25,50]). This heteroatom-substitution approach is now viewed as the easiest way to obtain xanthene analogs with spectral features in the red and/or far-red regions while keeping a small compact size, hydrophilic character and less propensity for aggregation-caused quenching (ACQ) [51] in aq. environment. Despite these benefits, our group has recently emphasized the poor aq. stability (at physiological pH) of silicon analog of 3-imino-3*H*-xanthen-6-amine, due to the marked

electrophilicity of its *meso*-position (*i.e.*, C-9 position of xanthene scaffold) which undergoes nucleophilic attack by a water molecule or a hydroxyde anion. Indeed, despite lower electronegativity of Si atom compared to O atom (1.9 against 3.5 in Linus Pauling's scale), the lack of electron-donating ability through +M effect seems to be critical in this regard [49]. To overcome this major issue that currently prevents symmetrical hetero-pyronins to find applications in sensing and bioimaging, desymmetrization of their core structure through the introduction of a tertiary aniline moiety with enhanced electron-donating ability, deserves to be explored.

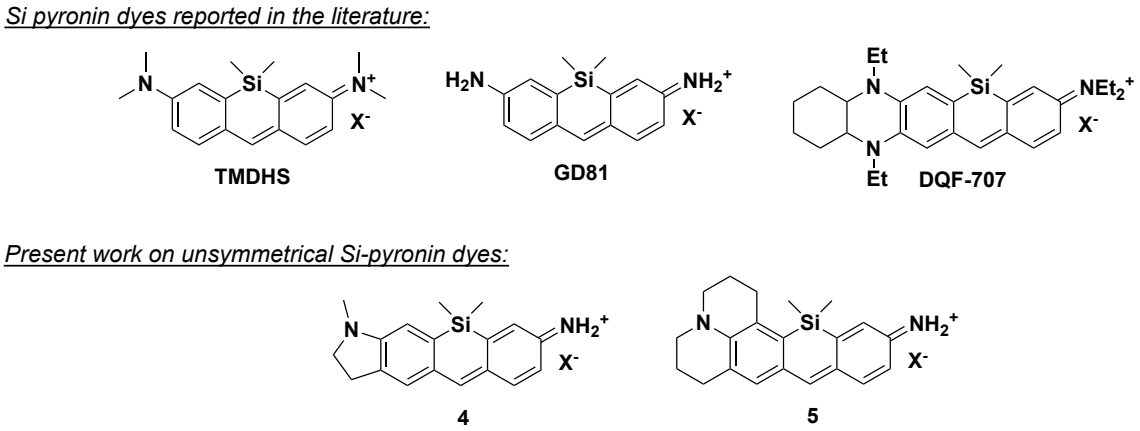

Fig. 2. Structures of Si-pyronin dyes already reported in the literature [44,48,49]; structures of unsymmetrical Si-pyronin dyes studied in the present work ($X = Cl^-$ for **TMDHS**, $X^- = CF_3CO_2^-$ for **GD81**, **4** and **5**, for **DQF-707**, the nature of X^- was not specified by the authors).

The present Article is put forward in that context. Indeed, we report the synthesis and photophysical characterizations of novel unsymmetrical pyronins **2** and **3** bearing both an optically tunable primary amino group and a tertiary aniline donor unit (Fig. 1). In addition, alternative synthetic routes have also been devised to their silicon analogs (Si-pyronins **4** and **5**, Fig. 2) finally subjected to a pH-dependent stability study aimed at identifying novel far-red fluorogenic molecules usable in physiological conditions.

2. Experimental

2.1. General

Unless otherwise noted, all commercially available reagents and solvents were used without further purification. TLC were carried out on Merck Millipore DC Kieselgel 60 F-254 aluminum sheets. The spots were directly visualized or through illumination with UV lamp (λ = 254/365 nm). Column chromatography purifications were performed on silica gel (40-63 μm

or 63-200 μm) from VWR. Some chromatographic purifications were performed using an automated flash chromatography purification system (Interchim puriFlash® 430) with puriFlash® columns (silica gel, 25 μm). THF (HPLC-grade, Fisher Chemical) was dried over alumina cartridges immediately priorv to use, by means of a solvent purification system PureSolv PS-MD-5 model from Innovative Technology. Anhydrous DMSO and 1,2-dichloroethane (DCE) were purchased from Carlo Erba and Sigma-Aldrich respectively, and stored over 3 Å molecular sieves. TFA was provided by Iris Biotech GmbH. The HPLC-gradient grade CH_3CN used for HPLC-MS analyses was obtained from Carlo Erba or VWR. Formic acid (FA, puriss p.a., ACS reagent, reag. Ph. Eur., ≥98%) was provided by Sigma-Aldrich. All aq. buffers used in this work and aq. mobile-phases for HPLC were prepared using water purified with a PURELAB Ultra system from ELGA (purified to 18.2 MΩ.cm). *sec*-Butyllithium (*sec*-BuLi) solution (ca. 1.3 M in cyclohexane/hexanes 92:8, v/v, Acros Organics) was titrated before using (colorimetric titration with menthol + 2,2'-bipyridine in dry THF) [52]. *N*-Methyl-5-carboxaldehyde-6-bromoindoline [1428258-90-5], *N*-Boc-3-aminophenol [19962-06-2] and *N*-Boc-3-iodoaniline [143390-49-2] were prepared according to literatures procedures [42,53-55].

2.2. Instruments and methods

^{1}H-, ^{13}C-, ^{19}F- and ^{29}Si-NMR spectra were recorded either on a Bruker Avance III 400 MHz or 500 MHz or on a Bruker Avance III HD 600 MHz spectrometer (equipped with double resonance broad band probes). Chemical shifts are expressed in parts per million (ppm) from the residual non-deuterated solvent signal [56]. *J* values are expressed in Hz. IR spectra were recorded with a Bruker Alpha FT-IR spectrometer equipped with an universal ATR sampling accessory. The bond vibration frequencies are expressed in reciprocal centimeters (cm^{-1}). HPLC-MS analyses were performed on a Thermo-Dionex Ultimate 3000 instrument (pump + autosampler at 20 °C + column oven at 25 °C) equipped with a diode array detector (Thermo-Dionex DAD 3000-RS) and MSQ Plus single quadrupole mass spectrometer. Purifications by semi-preparative HPLC were performed on a Thermo-Dionex Ultimate 3000 instrument (semi-preparative pump HPG-3200BX) equipped with a RS Variable Detector (VWD-3400RS, four distinct wavelengths within the range 190-900 nm). Lyophilization steps were performed with a Christ Alpha 2-4 LD plus. Ion chromatography analyses (for TFA quantification) were performed using an ion chromatograph Thermo Scientific Dionex ICS 5000 equipped with a conductivity detector CD (Thermo Scientific Dionex) and a conductivity suppressor ASRS-

ultra II 4 mm (Thermo Scientific Dionex). Low-resolution mass spectra (LRMS) were recorded on a Thermo Scientific MSQ Plus single quadrupole equipped with an electrospray (ESI) source (LC-MS coupling mode). UV-visible spectra were obtained either on a Varian Cary 50 Scan or on a Agilent Cary 60 (single-beam) spectrophotometer by using a rectangular quartz cell (Hellma, 100-QS, 45 × 12.5 × 12.5 mm, pathlength: 10 mm, chamber volume: 3.5 mL), at 25 °C (using a temperature control system combined with water circulation). Fluorescence spectra were recorded on an HORIBA Jobin Yvon Fluorolog spectrofluorometer (software FluorEssence) at 25 °C (using a temperature control system combined with water circulation), with a standard fluorometer cell (Labbox, LB Q, light path: 10 mm, width:10 mm, chamber volume: 3.5 mL). The absorption spectra of (Si-)pyronin dyes were recorded in the corresponding solvent with concentrations in the range 5-25 μM (three distinct dilutions for the accurate determination of molar extinction coefficients). Excitation/emission spectra were recorded after emission/excitation at the suitable wavelength (see Table 1, set of parameters for Fluorolog: shutter: Auto Open, excitation/emission slit = 5 nm, integration time = 0.1 s, 1 nm step, HV(S1) = 950 V). All fluorescence spectra were corrected. Relative fluorescence quantum yields were measured in the corresponding buffer at 25 °C by a relative method using the suitable standard (see Table 1, dilution by a factor ×30 between absorption and fluorescence measurements). The following equation was used to determine the relative fluorescence quantum yield:

$$\Phi_F(x) = (A_S/A_X)(F_X/F_S)(n_X/n_S)^2\Phi_F(s)$$

where A is the absorbance (in the range of 0.01-0.1 A.U.), F is the area under the emission curve, n is the refractive index of the solvents (at 25 °C) used in measurements, and the subscripts s and x represent standard and unknown, respectively.

Table 1. Experimental conditions used for the determination of relative fluorescence quantum yield.

Fluorophore[a]	Solvent[b]	λ Ex (nm)[c]	Standard (std)	$\Phi_{F(std)}$ / solvent	Φ_F
2	PBS, pH 7.6	500	R6G	0.76 / H_2O[d] [57]	0.76
3	PBS, pH 7.6	520	Rh101	1.00 / MeOH[d] [57]	0.72
4	PBS, pH 7.5	545	SR101	0.95 / EtOH[d] [57]	0.27
5	PBS, pH 7.5	545	SR101	0.95 / EtOH[d] [57]	0.42

[a] stock solutions (1.0 mg/mL) of fluorophores were prepared either in spectroscopic grade DMSO.
[b] PBS = 100 mM phosphate + 150 mM NaCl, refractive index (PBS) = 1.337.
[c] emission range for **2** = 510-800 nm, emission range for **3** = 530-800 nm, emission range for **4** and **5** = 560-850 nm.
[d] refractive index (H_2O) = 1.333, refractive index (MeOH) = 1.328, refractive index (EtOH) = 1.361.

2.3. High-performance liquid chromatography separations

Several chromatographic systems were used for the analytical experiments and purification steps: *System A*: RP-HPLC (Phenomenex Kinetex C_{18} column, 2.6 µm, 2.1 × 50 mm) with CH_3CN (+ 0.1% FA) and 0.1% aq. formic acid (aq. FA, pH 2.5) as eluents [5% CH_3CN (0.1 min) followed by linear gradient from 5% to 100% (5 min) CH_3CN, then 100% CH_3CN (1.5 min)] at a flow rate of 0.5 mL/min. UV-visible detection was achieved at four distinct wavelengths in the range 220-700 nm (variables according to the compound to be analyzed + diode array detection in the range 220-800 nm). Low resolution ESI-MS detection in the positive/negative mode (full scan, 150-1500 a.m.u., peaking format: centroid, needle voltage: 3.0 kV, probe temperature: 350 °C, cone voltage: 75 V and scan time: 1 s). *System B*: semi-preparative RP-HPLC (SiliCycle SiliaChrom C_{18} column, 10 µm, 20 × 250 mm) with CH_3CN and 0.1% aq. TFA as eluents [0% CH_3CN (5 min), followed by a linear gradient from 0 % to 10 % (10 min) and 10 % to 100 % (115 min) of CH_3CN] at a flow rate of 20.0 mL/min. Quadruple UV-visible detection was achieved at 220, 245, 473 and 522 nm. *System C*: system B with the following gradient [0% CH_3CN (5 min), followed by a linear gradient from 10 % to 25% (15 min) and 25% to 85% (120 min) of CH_3CN] at a flow rate of 20.0 mL/min. Quadruple UV-visible detection was achieved at 220, 315, 350 and 650 nm. *System D*: system B with the following gradient [15% CH_3CN (5 min), followed by a linear gradient from 15% to 30% (15 min) and 30% to 85% (124 min) of CH_3CN]. Quadruple UV-visible detection was achieved at 250, 280, 350 and 620 nm. *System E*: semi-preparative RP-HPLC (Thermo Hypersil GOLD C_{18} column, 5 µm, 10 × 250 mm) with CH_3CN and 0.1% aq. TFA as eluents [15% CH_3CN (5 min), followed by a linear gradient from 15% to 25% (5 min) and 25% to 100% (105 min) of CH_3CN]

at a flow rate of 4.0 mL/min. Quadruple UV-visible detection was achieved at 250, 280, 350 and 620 nm.

2.4. Synthesis of unsymmetrical pyronin bearing N-methylindoline as donor unit

*2.4.1 Mixed bis-aryl ether (**7**)*

A mixture of *N*-Methyl-5-carboxaldehyde-6-bromoindoline (300 mg, 1.25 mmol, 1.0 equiv.), *N*-Boc-3-aminophenol (444 mg, 2.12 mmol, 1.7 equiv.), finely ground K_3PO_4 (531 mg, 2.5 mmol, 2 equiv.), CuI (24 mg, 0.125 mmol, 0.1 equiv.) and picolinic acid (31 mg, 0.25 mmol, 0.2 equiv.) in dry DMSO (3 mL) was heated in a sealed tube at 90 °C overnight. The reaction was checked for completion by TLC (heptane-EtOAc 8:2, v/v) and diluted with EtOAc. Then, the resulting mixture was washed with deionized H_2O three times and brine, dried over anhydrous $MgSO_4$, filtered and concentrated under reduced pressure. The resulting residue was purified by flash-column chromatography over silica gel (eluent: step gradient of EtOAc in heptane from 10% to 30%) to obtained the compound **7** (136 mg, 0.38 mmol, yield 30%) as a yellow amorphous powder. IR (ATR): ν 644, 686, 727, 772, 817, 879, 906, 941, 969, 981, 998, 1060, 1150, 1233, 1268, 1287, 1342, 1366, 1384, 1438, 1474, 1492, 1520, 1577, 1597, 1653, 1722, 2248, 2852, 2927, 2974, 3300; ^{1}H NMR (500 MHz, $CDCl_3$): δ 10.08 (s, 1H, H-aldehyde), 7.55 (t, J = 1.2 Hz, 1H), 7.23 (t, J = 8.3 Hz, 1H), 7.17-7.13 (m, 2H), 6.68 (ddd, J = 8.3 Hz, J = 2.2 Hz, J = 1.2 Hz, 1H), 6.63 (s, 1H), 5.74 (s, 1H), 3.54 (t, J = 8.5 Hz, 2H), 2.98 (td, J = 8.5 Hz, J = 1.4 Hz, 2H), 2.76 (s, 3H), 1.49 (s, 9H, CH_3-Boc); ^{13}C NMR (126 MHz, $CDCl_3$): δ 187.0, 162.8, 159.1, 158.0, 152.7, 140.1, 130.2, 125.9, 123.0, 117.1, 113.7, 113.2, 109.3, 94.9, 80.9, 55.1, 33.9, 28.4, 26.9; HPLC (system A): t_R = 5.2 min (purity 93% at 260 nm); LRMS (ESI+, recorded during RP-HPLC analysis): *m/z* 313.3 $[M - t\text{Bu} + H]^+$ (90), 369.2 $[M + H]^+$ (100), 737.3 $[2M + H]^+$ (10), calcd for $C_{21}H_{25}N_2O_4^+$ 369.2; LRMS (ESI-, recorded during RP-HPLC analysis): *m/z* 366.8 $[M - H]^-$ (80), 413.3 $[M + FA - H]^-$ (100), 781.1 $[2M + FA - H]^-$ (55), calcd for $C_{21}H_{24}N_2O_4^-$ 367.2.

*2.4.2 Unsymmetrical pyronin (**2**)*

Mixed bis-aryl ether **7** (80 mg 0.22 mol, 1 equiv.) was dissolved in 55:45 (v/v) TFA-DCM mixture (1.25 mL). The mixture was stirred at room temperature for 2 h and at 55 °C for 21 h. The reaction was checked for completion by TLC (DCM-MeOH 9:1, v/v). Thereafter, the reaction mixture was concentrated under reduced pressure. The resulting residue was purified

by flash-column chromatography over silica gel (eluent: step gradient of MeOH in DCM from 0% to 10%) to give 25.5 mg of the desired xanthene dye (yield 31%). A further purification was achieved by semi-preparative HPLC (system B, t_R = 29.0-34.0 min) to obtain pyronin **2** with the optimal purity suitable for photophysical characterizations (>95%). TFA salt of **2** was recovered (after freeze-drying) as a red amorphous powder (10 mg, 27 μmol, yield 12%, based on mass of TFA = 34.4% determined by ionic chromatography). IR (ATR): ν 610, 628, 651, 677, 716, 727, 741, 775, 798, 826, 844, 877, 931, 959, 982, 1123, 1168, 1198, 1299, 1323, 1338, 1380, 1411, 1516, 1541, 1575, 1601, 1620, 1655, 1669, 1683, 1799, 1997, 2012, 2166, 2188, 2311, 2359, 2421, 2811, 2934, 3124, 3282, 3320; ^{1}H NMR (500 MHz, CD_3OD): δ 8.36 (s, 1H), 7.65 (d, J = 8.8 Hz, 1H), 7.41 (s, 1H), 6.91 (dd, J = 8.7 Hz, J = 2.0 Hz, 1H), 6.74 (s, 1H), 6.61 (s, 1H), 3.96 (t, J = 7.6 Hz, 2H), 3.23 (t, J = 7.6 Hz, 2H), 3.19 (s, 3H); ^{13}C NMR (126 MHz, CD_3OD): δ 162.9, 161.8, 160.3, 159.0, 145.4, 135.9, 134.0, 126.3, 117.4, 117.3, 114.8, 98.34, 91.6, 56.2, 33.7, 30.7, 26.8, 24.2; ^{19}F NMR (470 MHz, CD_3OD): δ -76.9 (s, 3F, C*F*$_3$-TFA); HPLC (system A): t_R = 3.4 min (purity 99% at 260 nm, >99% at 450 nm and >99 % at 500 nm); LRMS (ESI+, recorded during RP-HPLC analysis): *m/z* 251.3 $[M + H]^+$ (100), calcd for $C_{16}H_{15}N_2O^+$ 251.1.

2.5. Synthesis of unsymmetrical pyronin bearing julolidine as donor unit

*2.5.1 Mixed bis-aryl ether (**8**)*

A mixture of commercial 8-hydroxyjulolidine 9-carboxaldehyde (638 mg, 2.94 mmol, 1.7 equiv.), *N*-Boc-3-iodoaniline (552 mg, 1.73 mmol, 1 equiv.), finely ground K_3PO_4 (732 mg, 3.45 mmol, 2 equiv.), CuI (33 mg, 0.17 mmol, 0.1 equiv.) and picolinic acid (43 mg, 0.35 mmol, 0.2 equiv.) in dry DMSO (4.2 mL) was heated in a sealed tube at 90 °C overnight. The reaction was checked for completion by TLC (DCM 100%) and diluted with EtOAc. Then, the resulting mixture was washed with deionized H_2O three times and brine, dried over anhydrous $MgSO_4$, filtered and concentrated under reduced pressure. The resulting residue was purified by flash-column chromatography over silica gel (eluent: step gradient of EtOAc in heptane from 10% to 20%) to obtained the compound **8** (247 mg, 0.63 mmol, yield 37%) as a yellow amorphous powder. IR (ATR): ν 656, 685, 726, 768, 832, 860, 905, 956, 980, 1006, 1049, 1070, 1129, 1148, 1197, 1235, 1269, 1281, 1306, 1341, 1366, 1390, 1454, 1492, 1519, 1589, 1652, 1722, 2058, 2249, 2843, 2933, 2843, 3294; ^{1}H NMR (500 MHz, $CDCl_3$): δ 9.82 (s, 1H, H-aldehyde), 7.42 (d, J = 1.0 Hz, 1H), 7.13 (t, J = 8.2 Hz, 1H), 7.04 (d, J = 8.2 Hz, 1H), 6.89 (t, J = 2.2 Hz, 1H), 6.53 (s, 1H), 6.46-6.42 (m, 1H), 3.28 (dd, J = 6.6 Hz, J = 4.9 Hz, 2H), 3.23 (dd, J = 6.6

Hz, J = 4.9 Hz, 2H), 2.75 (t, J = 6.3 Hz, 2H), 2.50 (t, J = 6.3 Hz, 2H), 2.03-1.91 (m, 2H), 1.89-1.78 (m, 2H), 1.48 (s, 9H, CH_3-Boc); ^{13}C NMR (126 MHz, $CDCl_3$): δ 187.5, 159.8, 154.3, 152.6, 149.4, 140.1, 130.2, 126.5, 118.3, 117.1, 112.6, 112.1, 109.4, 105.7, 80.8, 50.2, 49.8, 28.4, 27.5, 21.4, 21.1, 20.6; HPLC (system A): t_R = 5.5 min (purity 97 % at 260 nm); LRMS (ESI+, recorded during RP-HPLC analysis): *m/z* 353.2 $[M - tBu + H]^+$ (100), 409.4 $[M + H]^+$ (60), 817.5 $[2M + H]^+$ (5), calcd for $C_{24}H_{29}N_2O_4^+$ 409.2; LRMS (ESI-, recorded during RP-HPLC analysis): *m/z* 453.3 $[M + FA - H]^-$ (100), calcd for $C_{25}H_{29}N_2O_6^-$ 453.2.

*2.5.2 Unsymmetrical pyronin (**3**)*

Mixed bis-aryl ether **8** (100 mg 0.25 mmol, 1 equiv.) was dissolved in 55:45 (v/v) TFA-DCM mixture (1.6 mL). The mixture was stirred at room temperature for 30 min. The reaction was checked for completion by TLC (DCM-MeOH 9:1, v/v). Thereafter, the reaction mixture was concentrated under reduced pressure. The resulting residue was purified by flash-column chromatography over silica gel (eluent: step gradient of MeOH in DCM from 0% to 10%) to give 18 mg of the desired xanthene dye (yield 17%). A further purification was achieved by semi-preparative RP-HPLC to obtain pyronin **3** with the optimal purity suitable for photophysical characterizations (>95%). TFA salt of **3** was recovered (after freeze-drying) as a red amorphous powder (15.6 mg, 40 μmol, yield 16% based on mass of TFA = 34% determined by ionic chromatography). IR (ATR): ν 614, 648, 715, 734, 755, 797, 823, 843, 935, 973, 1029, 1042, 1118, 1158, 1194, 1307, 1324, 1342, 1364, 1412, 1445, 1501, 1529, 1580, 1598, 1654, 1685, 2854, 2944, 3093, 3320; ^{1}H NMR (500 MHz, CD_3OD): δ 8.21 (s, 1H), 7.57 (d, J = 8.8 Hz, 1H), 7.27 (s, 1H), 6.84 (dd, J = 8.8 Hz, J = 2.1 Hz, 1H), 6.67 (d, J = 2.1 Hz, 1H), 3.56 (t, J = 5.8 Hz, 4H), 2.91 (t, J = 6.3 Hz, 2H), 2.85 (t, J = 6.3 Hz, 2H), 2.03 (dt, J = 18.3 Hz, J = 5.9 Hz, 4H); ^{13}C NMR (126 MHz, CD_3OD): δ 160.4, 159.1, 154.1, 154.0, 145.4, 134.1, 129.9, 126.2, 116.9, 115.9, 114.6, 106.40, 98.4, 52.3, 51.7, 28.3, 21.6, 20.5, 20.5; ^{19}F NMR (470 MHz, CD_3OD): δ -76.9 (s, 3F, C*F*$_3$-TFA). HPLC (system A): t_R = 3.9 min (purity >99% at 260 nm, >99% at 450 nm and >99% at 500 nm). LRMS (ESI+, recorded during RP-HPLC analysis): *m/z* 291.3 $[M + H]^+$ (100), calcd for $C_{19}H_{19}N_2O^+$ 291.3.

2.6. Synthesis of unsymmetrical Si-pyronin bearing N-methylindoline as donor unit

*2.6.1 N,N-Diallyl Si-pyronin (**14**)*

To a solution of bis(bromoaryl) derivative **12** (see ESI for its synthesis, 444 mg, 0.93 mmol, 1 equiv.) in dry THF (20 mL) was added slowly *sec*-BuLi (2.05 mL, 2.15 mmol, 2.3 equiv.) at -78 °C under argon atmosphere. The resulting reaction mixture was stirred for 30 min at the same temperature and then dichlorodimethylsilane (Me_2SiCl_2, 259 µL, 2.15 mmol, 2.3 equiv.) in dry THF (8 mL) was added slowly at 0 °C. The reaction mixture was stirred at -12 °C for 20 min and then allowed to warm to room temperature and stirred for 1 h. Thereafter, the reaction mixture was quenched with sat. aq. sat. NH_4Cl (10 mL) and extracted with DCM (3 × 50 mL). The combined organic layers were dried over anhydrous Na_2SO_4, filtered and finally concentrated under reduced pressure. The resulting residue was dissolved in DCM (10 mL) and DDQ (212 mg, 0.93 mmol, 1 equiv.) was added. The aromatization reaction was found to be complete within 20 min as indicated by the rapid appearance of an intense blue color, the reaction was checked for completion by RP-HPLC (system A). Thereafter, the organic layer was washed with aq. $NaHCO_3$ (pH 7.5-8.0) (3 × 60 mL), brine, dried over anhydrous Na_2SO_4 and concentrated under reduced pressure. Purification was done by automated flash-column chromatography with a silica gel cartridge (25 g, 25 µm, eluent: step gradient of EtOAc in heptane from 50% to 100%, over 2 h) to give an unresolved mixture of the desired product **14**, Si-xanthone and a residual amount of DDQ. *Please note: to prevent complete oxidation of Si-pyronin into Si-xanthone, the crude mixture was used without further purification in the next step*. HPLC (system A): t_R = 4.7 min; LRMS (ESI+, recorded during RP-HPLC analysis): *m/z* 373.2 $[M]^{+\circ}$, calcd for $C_{24}H_{29}N_2Si^+$ 373.2; UV-vis (recorded during RP-HPLC analysis): λ_{max} 320 and 652 nm. For Si-xanthone derivative: HPLC (system A): t_R = 4.2 min; LRMS (ESI+, recorded during RP-HPLC analysis): *m/z* 389.2 $[M + H]^+$, calcd for $C_{24}H_{29}N_2OSi^+$ 389.2; UV (recorded during RP-HPLC analysis): λ_{max} 251, 291 and 353 nm.

*2.6.2 Unsymmetrical Si-pyronin (**4**)*

Impure *N*,*N*-diallyl Si-pyronin **14** (133 mg) and 1,3-dimethylbarbituric acid (112 mg, 0.72 mmol, 2 equiv., based on 0.35 mmol of **14** theoretically obtained with a quantitative yield for the previous step) were dissolved in degassed DCE (15 mL). Catalytic amount of $Pd(PPh_3)_4$ (58 mg, 50 µmol, 0.14 equiv.) was added and the resulting reaction mixture was stirred at 35 °C for 45 min. The reaction was checked for completion by RP-HPLC (system A). Thereafter, the organic layer was washed with deionized H_2O (50 mL), brine, dried over anhydrous Na_2SO_4 and concentrated under reduced pressure. The resulting residue was dissolved in a 1:1 mixture of 0.1% aq. TFA and CH_3CN and purified by semi-preparative RP-HPLC (system C). The

product-containing fractions (t_R = 35.0-39.2 min) were lyophilized to give **4** as a bluish-purple amorphous powder (23 mg, 55 μmol, overall yield 6% for the two steps and based on mass of TFA = 31% determined by ionic chromatography). IR (ATR): ν 3320, 3123 (broad), 1686, 1658, 1624, 1592, 1543, 1516, 1500, 1475, 1450, 1415, 1396, 1354, 1321, 1283, 1187, 1156 (broad), 1124, 1112, 1058, 1025, 654, 605, 828, 799, 779, 749, 718, 697, 665, 597, 501, 418, 396; ^{1}H NMR (500 MHz, CD_3CN): δ 7.60 (s, 1H), 7.50 (d, J = 8.6 Hz, 1H), 7.31 (s, 1H), 7.14 (d, J = 2.5 Hz, 2H), 6.77 (dd, J = 8.6 Hz, J = 2.5 Hz, 1H), 3.95 (t, J = 7.6 Hz, 2H), 3.25 (s, 3H), 3.11 (t, J = 7.6 Hz, 2H) 0.45 (s, 6H); ^{13}C NMR (126 MHz, CD_3CN): δ 160.4, 158.3, 155.9, 153.8, 146.1, 142.8, 136.7, 135.4, 130.0, 128.6, 123.2, 116.2 (2C), 56.2, 34.5, 26.3, -1.6 (2 C, Si(CH_3)$_2$); ^{19}F NMR (470 MHz, CD_3CN): δ -75.8 (s, 3F, CF_3-TFA); ^{29}Si NMR (99 MHz, CD_3CN): δ -18.1 (s, 1Si, *Si*(CH_3)$_2$). HPLC (system A): t_R = 3.8 min (purity >98% at 300 nm and >99% at 650 nm); UV-vis (recorded during the HPLC analysis): λ_{max} 313 and 629 nm; LMRS (ESI+, recorded during RP-HPLC analysis): *m/z* 293.3 $[M + H]^+$, calcd for $C_{18}H_{21}N_2Si^+$ 293.1;

2.7. Synthesis of unsymmetrical Si-pyronin bearing julolidine as donor unit

*2.7.1 N,N-Diallyl Si-pyronin (**15**)*

To a solution of bis(bromoaryl) derivative **13** (see ESI for its synthesis, 530 mg, 1.03 mmol, 1 equiv.) in dry THF (40 mL) was added slowly *sec*-BuLi (2.15 mL, 2.57 mmol, 2.5 equiv.) at -78°C under argon atmosphere. The resulting reaction mixture was stirred for 1 hour at the same temperature and then Me_2SiCl_2 (337 μL, 2.8 mmol, 2.8 equiv.) in dry THF (10 mL) was added slowly at -15 °C. The reaction mixture was stirred at -15 °C for 20 min and then allowed to warm to room temperature and stirred for 1 h. Thereafter, the reaction mixture was quenched with aq. sat. NH_4Cl (10 mL) and extracted with DCM (4 × 40 mL). The combined organic layers were dried over anhydrous Na_2SO_4, filtered and finally concentrated under reduced pressure. The resulting residue was dissolved in DCM (30 mL) and DDQ (227 mg, 1.0 mmol, 0.9 equiv.) was added. The aromatization reaction was found to be complete within 20 min as indicated by the rapid appearance of an intense blue color, the reaction was checked for completion by RP-HPLC (systeme A). Thereafter, the organic layer was washed with aq. $NaHCO_3$ (pH 7.5-8.0) (50 mL), brine, dried over anhydrous Na_2SO_4 and concentrated under reduced pressure. HPLC (system A): t_R = 4.9 min; LMRS (ESI+, recorded during RP-HPLC analysis): *m/z* 413.3 $[M]^{+\circ}$, calcd for $C_{27}H_{33}N_2Si^+$ 413.2; UV-vis (recorded during RP-HPLC analysis): λ_{max} 321 and 644

nm. *Please note: due to the propensity of this Si-pyronin to be rapidly oxidized to Si-xanthone, the mixture was used in the next step without further purification.*

*2.7.2 Unsymmetrical Si-pyronin (**5**)*

Impure *N*,*N*-diallyl Si-pyronin **15** (425 mg) and 1,3-dimethylbarbituric acid (321 mg, 2.06 mmol, 2 equiv., based on 1.03 mmol of **15** theoretically obtained with a quantitative yield for the previous step) were dissolved in degassed DCE (50 mL). $Pd(PPh_3)_4$ (178 mg, 150 μmol, 0.15 equiv.) was added and the resulting reaction mixture was stirred at room temperature. The reaction was checked for completion by RP-HPLC (system A). Thereafter, the organic layer was washed with deionized H_2O (50 mL), brine, dried over anhydrous Na_2SO_4 and concentrzted under reduced pressure. The resulting residue was dissolved in a 1:2 mixture of 0.1% aq. TFA and CH_3CN and purified by semi-preparative RP-HPLC (system D, six distinct injections). A first pure sample of Si-pyronin **5** (t_R = 44.5-45.5 min) was recovered as TFA salt after freeze-drying (dark purple amorphous powder, 7.3 mg). The combined batches of lower purity was subjected to a second RP-HPLC purification (system E). The product-containing fractions (t_R = 30.3-31.2 min) were lyophilized to give a further amount (ca. 2 mg) of **5** (10 mg, 20 μmol, overall yield 2% for the two steps and based on mass of TFA = 34% determined by ionic chromatography). HPLC (system A): t_R = 4.2 min (purity >99% at 300 nm and >99% at 650 nm); UV-vis (recorded during the HPLC analysis): λ_{max} 303 and 623 nm; LMRS (ESI+, recorded during RP-HPLC analysis): *m/z* 333.2 $[M + H]^+$, calcd for $C_{21}H_{25}N_2Si^+$ 333.2. *Please note: purity control by RP-HPLC-MS of Si-pyronin **5** was achieved few days after isolation/lyophilization of this compound and a stock solution in DMSO (1.0 mg/mL) was prepared and used for photophysical characterizations. However and unfortunately, full spectroscopic characterization of this fluorophore through NMR measurements was not completed immediately, and an unexpected TFA-mediated degradation occurring at the solid state and despite storage at 4 °C, has led to the loss of this product.*

2.8 Determination of the equilibrium constant related to aq. stability of Si-pyronin dyes

Stock solution of Si-pyronins (TFA salt) **4** and **5** was prepared in spectroscopic grade DMSO (1.0 mg/mL, 2.9 mM and 2.1 mM respectively). Each compound was incubated in the corresponding buffer (NaOAc, PB, borate or carbonate-bicarbonate buffer to cover the pH range 3.5-10.9) at 23 °C (temperature of air-conditioned lab) for 15 min (concentration: 5.0 μM

and 3.5 μM respectively, 5 μL of stock solution in 3 mL of buffer). Thereafter, visible absorption spectrum (400-700 nm) of each solution was recorded at 25 °C. The absorbance at λ_{max} = 626 nm or 620 nm was noted and plotted versus the buffer pH value. Curve fitting was achieved with OriginPro 8 software (fit sigmoidal, Boltzmann function) that also provided the inflection point whose the x-coordinate corresponds to the pK of the equlibrium dye-pseudobase.

3. Results and discussion

3.1. Synthesis of unsymmetrical pyronin dyes bearing a tertiary aniline unit

Prior to the present work, and to our knowledge, only three examples of unsymmetrical pyronin dyes have been described in the literature, **1** [24], **DQF594** [44] and **AR116** [40] (Fig. 1). $MeSO_3H$- or TFA-mediated condensation reaction between 4-(diethylamino)salicylaldehyde and the corresponding 3-aminophenol/*meta*-anisidine derivative directly provided the corresponding xanthene-based fluorophore. Unfortunately, for **AR116**, both conversion rate and isolated yield are very poor due to (1) the preferred formation of imine derivative upon reaction between aldehyde and primary aniline and (2) purification difficulties linked to minor differences in polarity between **AR116** and starting 4-(diethylamino)salicylaldehyde. To overcome these problems, we recently developed an efficient alternative synthetic route to **AR116**, inspired by the work of Anzalone *et al.* on the gram scale synthesis of oxazine and xanthene fluorophores [58]. This method is based on a two-step synthesis starting from a copper-catalyzed Ullmann-type C-O cross-coupling reaction between 4-(diethylamino)salicylaldehyde and *N*-Boc-3-iodoaniline, followed by an unprecedented TFA-mediated domino deprotection/cylization/aromatization reaction (isolated overall yield 14% vs. <2% for one-step protocol). The advantages of this are multiple: (1) facile isolation of the intermediate mixed bis-aryl ether through flash-column chromatography over silica gel, that avoids possible contamination of **AR116** with starting salicylaldehyde, (2) ease of implementation even at large scale with cheap reagents and (3) versatility due to the broad scope of bis-aryl ether synthesis under Ullmann conditions. With the twin goals of demonstrating the potential of this synthesis approach and improving spectral features (especially fluorescence quantum yield) of fluorogenic pyronin dye **AR116**, we applied this

effective two-step protocol to the preparartion of two analogs bearing *N*-methylindoline or julolidine moiety instead of *N*,*N*-diethylaniline fragment (Fig. 1).

As depicted in Scheme 1, *N*-methylindoline pyronin dye **2** was readily obtained from *N*-methyl-5-carboxaldehyde-6-bromoindoline **6** and *N*-Boc-3-aminophenol. Ullmann-type reaction was achieved under conditions previously optimized and the targted mixed bis-aryl ether **7** was easily isolated in a pure form and with a moderate 30% yield. Prolonged incubation (21 h) of **7** in TFA-DCM (55:45, v/v) at 55 °C was identified as the conditions most suited to perform Boc-deprotection/cyclization/aromatization cascade reaction leading to unsymmetrical pyronin dye **2**. Once again, facile chromatographic isolation over silica gel column provided **2** with a satisfying purity. Optimal purity (>95%) required for photophysical measurements was readily achieved by further purification by semi-preparative RP-HPLC. The synthetic access to julolidine pyronin dye **3** was further facilitated by the commercial availability of one coupling partner assumed to be reactive in Ullmann-type cross-coupling: 8-hydroxyjulolidine-9-carboxaldehyde. Unlike the former synthesis (*vide supra*), the presence of reactive phenol moiety in this latter molecule involved the use of a *meta*-halogenoaniline as the second coupling reaction partner (instead of *meta*-hydroxyaniline for synthesis of **7**). Thus, *N*-Boc-3-iodoaniline was reacted with 8-hydroxyjulolidine-9-carboxaldehyde under the same conditions as those employed for synthesizing **7**. The resulting mixed bis-aryl ether **8** was next subjected to the acidic conditions TFA-DCM (9:7, v/v) found to be effective for its conversion to pyronin dye **3**. Gratifyingly, we noted that the reaction is complete within 30 min without requiring heating.

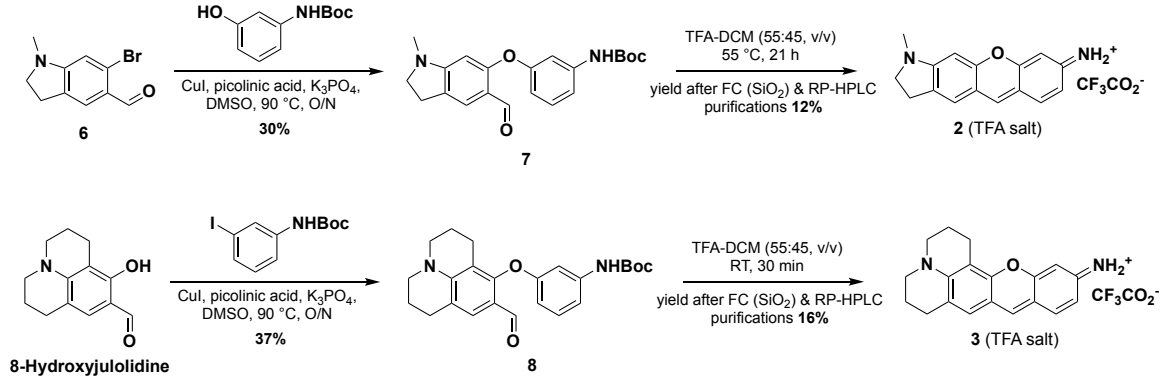

Scheme 1. Synthesis of unsymmetrical pyrionin dyes **2** and **3** (FC (SiO_2) = flash-column chromatography over silica gel, O/N = overnight, RT = room temperature).

The marked difference between **2** and **3** in the efficacy of intramolecular cyclization/dehydration domino process (after Boc removal) may be explained by superior rigidity of julolidine fragment that favors a coplanar structure for bis-aryl ether intermediate and hence the spatial proximity between reactive formyl group and phenylogous amine [59].

As in the case of **2**, twice chromatographic purifications (flash-chromatography over silica gel followed by semi-preparative RP-HPLC) gave unsymmetrical pyronin dye **3** in a pure form (>95%), as a TFA salt and with an isolated yield of 16%. All spectroscopic data (see ESI for the corresponding spectra, Figs. S6-S13 and S20-S27), especially IR, NMR and mass spectrometry, were in agreement with the structures assigned. The purity of pyronin samples was confirmed by RP-HPLC analyses with UV-vis detection at different wavelengths. Mass percentage of TFA in pyronin samples was determined by ionic chromatography (see ESI for the results, Figs. S14 and S28).

3.2. Synthesis of unsymmetrical Si-pyronin dyes bearing a tertiary aniline unit

To the best of our knowledge, there is only one example of unsymmetrical Si-pyronin dye described in the literature, *i.e.*, the silicon analog of **DQF594** (*vide supra*), named **DQF707** and published during the course of our work [44]. All synthetic strategies towards Si-xanthene dyes such as **DQF707**, symmetrical Si-pyronin **GD81**, Si-fluoresceins, Si-rhodamines and Si-rosamines are always based on the Hitchcock reaction (*i.e.*, bis-lithiation of a bis(bromoaryl) derivative and subsequent trapping with $SiMe_2Cl_2$) as the key step [60,61]. To apply this popular methodology to the preparation of silicon analogs of *N*-methylindoline- and julolidine-based pyronin dyes **4** and **5**, synthetic efforts must be focused on unsymmetrical bis(bromoaryl) derivatives **12** and **13**. Synthetic routes to these latter two key synthons are summarized in Schemes 2 and 3.

Firstly, on the one hand, the one-pot reduction and *N*-methylation (through reductive amination reaction) of commercial 6-bromoindole provided after conventional column chromatography over silica gel 6-bromo-1-methylindoline **9** in a satisfying 63% yield [62]. On the other hand, 8-bromojulolidine **10** was synthesized from 3-bromoaniline, which was reacted with 1-bromo-3-chloropropane (acting as both alkylating agent and solvent) with Na_2CO_3 at 140 °C overnight. Then, to achieve bis-cyclization through S_EAr reaction, DMF was added and the reaction mixture was stirred at 160 °C for 8 h [63]. **10** was recovered in a pure form by conventional flash-column chromatography over regular silica gel (yield 61%).

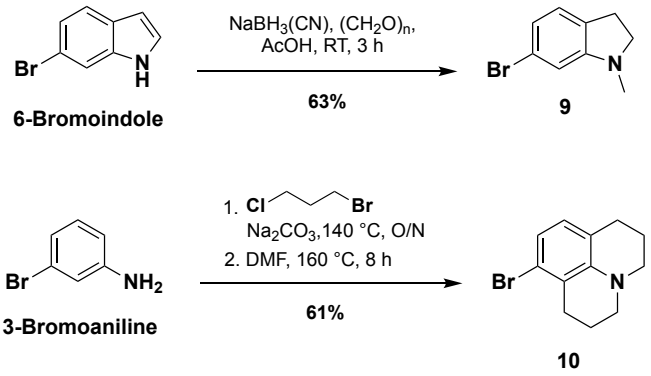

Scheme 2. Synthesis of *N*-methylindoline and julolidine derivatives **9** and **10** (AcOH = glacial acetic acid, RT = room temperature, O/N = overnight).

The next step was the formation of the unsymmetrical bis(bromoaryl) derivatives **12** and **13** through a Friedel-Crafts alkylation reaction between 6-bromo-1-methylindoline **9** (or 8-bromojulolidine **10**) and a benzyl-type cation generated from 4-(diallylamino)-2-bromobenzyl alcohol **11** (see ESI for its synthesis) in the presence of BF_3•Et_2O in DCM [64]. This reaction provided **12** and **13** in good reproducible yields (86% and 80% respectively). Concerning the practical implementation of sophisticated Hitchcock reaction, it is important to note that the formation of dilithiated anion intermediate was found to be slower for the julolidine-based bis(bromoaryl) derivative **13** (1 h instead of 30 min for *N*-methylindoline counterpart). This may be explained by higher steric hindrance of julolidine moiety. Moreover, the reaction mixture temperature at which $SiMe_2Cl_2$ was added, has been identified as a critical point for the success of the reaction. Several attempts were required to find the right temperature for each of the two compounds: 0 °C for reaction conducted with *N*-methylindoline derivative **12** and -15 °C for the julolidine counterpart **13**. Thereafter, the resulting Si-dihydropyronin derivatives were rapidly oxidized with DDQ (less than 15 min) to afford, in both cases, bluish-purple colored *N,N*-diallyl Si-pyronin dyes **14** and **15**. To avoid premature degradation of these fluorophores (observed during our initial attempts), crude reaction mixture were directly subjected to Tsuji-Trost de-allylation conditions [49,65]. Thus, final deprotection step was achieved by treatment of **14** and **15** with cat. amount of $Pd(PPh_3)_4$ and a large excess of 1,3-dimethylbarbituric acid (1,3-DMBA) in degassed DCE at 35 °C for 45 min for *N*-methylindoline-based Si-pyronin **4** and at room temperature for 80 min for julolidine-based Si-pyronin **5**. For both compounds, purification was achieved by semi-preparative RP-HPLC and several elution conditions have been sequentially applied for each sample to recover the desired unsymmetrical Si-pyronin dyes **4** and **5** in a pure form (>95%). This is why poor values of isolated yields (6% and 2% respectively) are not actually representative of the combined

conversion rates observed for the four-step process (bis-lithiation, silylation, aromatization and de-allylation). Spectroscopic data collected for these Si-xanthene derivatives (see ESI for the corresponding spectra, Figs. S31-S37 and S41-S42) were in agreement with the structures assigned. The purity of Si-pyronin samples was confirmed by RP-HPLC analyses with UV-vis detection at different wavelengths. Mass percentage of TFA in pyronin samples was again determined by ionic chromatography (see ESI for the results, Figs. S38 and S43). Curiously, we found that TFA salt of julolidine-based Si-pyronin dye **5** is not stable under solid form, even during storage at 4 °C while no degradation was not observed for its stock solutions (1.0 mg/mL) prepared in DMSO and stored at room temperature or in the fridge during long periods. This means that a counter-ion exchange process will have to be implemented prior to the long-term storage of this valuable fluorophore.

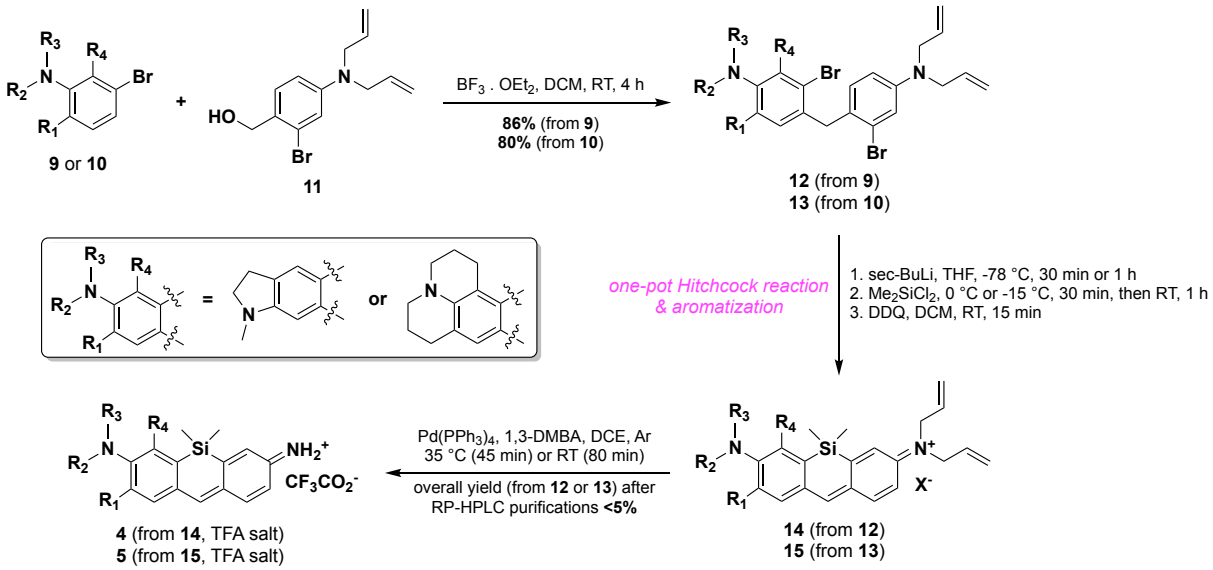

Scheme 3. Synthesis of unsymmetrical Si-pyronin dyes **4** and **5** (Ar = argon atmosphere, DCE = 1,2-dichloroethane, DDQ = 2,3-dichloro-5,6-dicyano-1,4-benzoquinone, 1,3-DMB = 1,3-dimethylbarbituric acid, RT = room temperature).

*3.3 Aqueous stability and photophysical characterization of pyronin dyes **2** and **3** and their silicon analogs **4** and **5***

Biosensing/bioimaging applications envisioned for reaction-based fluorescent probes based on fluorogenic primary anilines such as (Si-)pyronins presently developed, generally involve to work under physiological conditions. Therefore, the photophysical properties of compounds **2-5** were determined in phosphate buffered saline (PBS, 100 mM + 150 mM NaCl, pH 7.5) together with the known pyronin dyes 3-imino-3*H*-xanthen-6-amine and **AR116** already

synthesized by our group [49]. Table 2 provides the corresponding spectral features and the overlayed absorption/excitation/emission profiles are displayed in Fig. 3.

Table 2. Photophysical properties of 3-imino-3*H*-xanthen-6-amine (pyronin), **AR116** and (Si-)pyronin fluorophores studied in this work, determined in PBS at 25 °C.

Fluorophore[a]	λ Abs (nm)[b]	λ Em (nm)	ε (M^{-1} cm^{-1})	Stokes shift (cm^{-1})	Φ_F[c]
pyronin	496	514	81 400	706	0.92
AR116	527	548	64 800	727	0.06
2	519	540	66 800	749	0.76
3	540	561	57 400	693	0.72
4	625	651	47 200	639	0.27
5	620	640	40 600	504	0.42

[a] stock solutions (1.0 mg/mL) of fluorophores were prepared either in spectroscopic grade DMSO.
[b] only 0-0 band of the S0→S1 transition is reported.
[c] for experimental conditions used for such determination, see Table 1 and references [40,49].

All novel (Si-)pyronins display a broad and intense absorption band with a maximum in the range 520-625 nm, depending on the bis(amino)xanthene substitution pattern and the nature of intracyclic heteroatom, and assigned to the 0-0 band of the S0→S1 transition. A less pronounced shoulder peak at the higher energy side is also observed and is attributed to the vibronic relaxation (the 0-1 vibrational band) of the same transition.

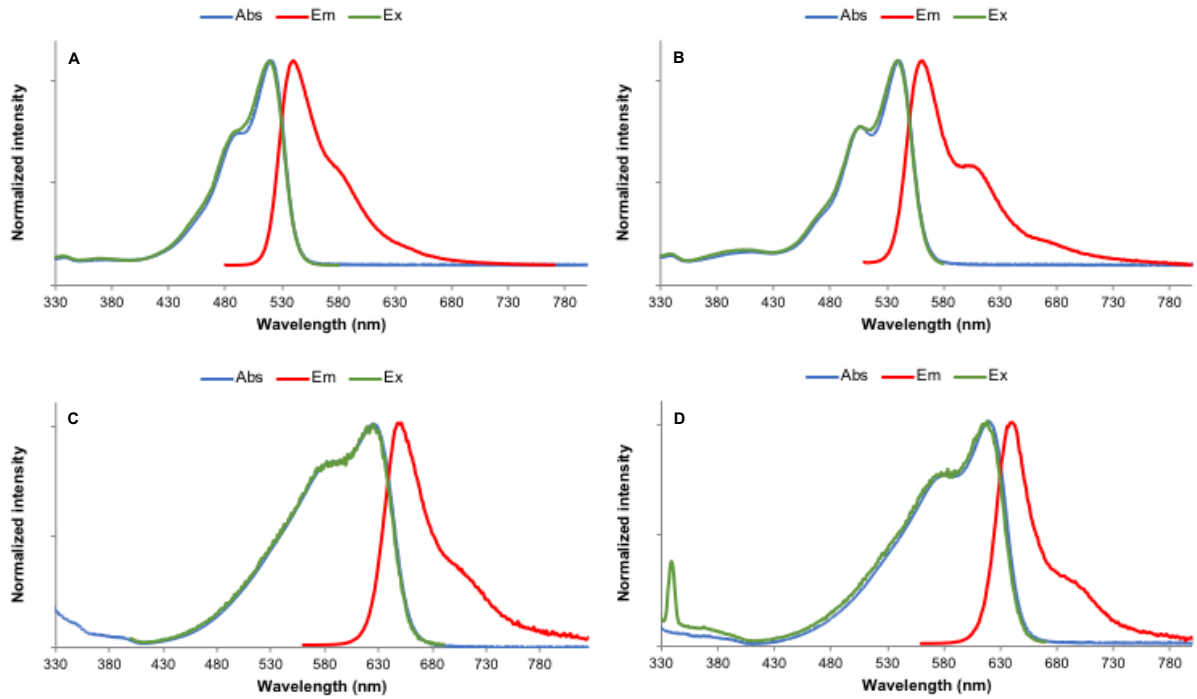

Fig. 3. Normalized absorption (blue), excitation (Em 600 nm for **2-3** or 710 nm for **4** or 680 nm for **4**, green) and emission (Ex 470 nm for **2**, 500 nm for **3** and 545 nm for **4-5**, red) spectra of unsymmetrical (Si-)pyronins **2** (A),

3 (B), **4** (C) and **5** (D) in PBS at 25 °C. *Please note: for the excitation spectrum of **5** in PBS, the peak at 340 nm ($\lambda_{EX}/2$) is assigned to Rayleigh scattering.*

In line with well-known features of rhodamines, the absorption maximum of pyronin scaffold is significantly red-shifted with an increasing electron-donating ability of the amino group of aniline fragment: $-NH_2$ < *N*-methylindoline ≃ $-NEt_2$ < julolidine. Since no study has ever compared absorption properties of a xanthene scaffold bearing either *N*-methylindoline or julolidine moieties as tertiary aniline units [66], the present work helps to show that the first one is less effective to cause a significant bathochromic shift and may even be regarded as a weaker electron donor than the conventional diethylamino group. Conversely, both *N*-methylindoline and julolidine moieties are known to readily promote rigidization of the core xanthene fluorophore bearing them, giving large increase in fluorescence quantum yield [59,62,64] as the result of reduced rotational or vibrational deactivation pathways of the excited state. This feature has been observed with the triptych **AR116**/**2**/**3**, as the Φ_F value changes from 7% to 72%-76% for an emission maximum being in the wavelength range 540-560 nm. Although unsymmetrical pyronin dyes **2** and **3** exhibit a more pronounced hydrophobic character, especially the julolidine derivative, no formation of non-emissive H-type aggregates occurred in neutral aq. solutions as evidenced by the perfect matching between the absorption and excitation spectra recorded in PBS, even at high concentrations in the range 5-20 μM.

Despite this tremendous improvement of fluorescence efficiency of the pyronin scaffold, the major limitation of these fluorogenic anilines is related to their absorption/emission maxima outside the far-red region or the NIR-I "therapeutic optical window" (*i.e.*, from 650 to 900 nm). Among the different possible molecular design strategies to obtain long-wavelength fluorescent analogs of xanthene dyes, the heteroatom-substitution approach historically proposed by the Qian group in 2008 [48], then studied in details by the Hanoka-Nagano-Urano group for preparing a set of practical Si-fluorescein, Si-rhodamine and Si-rosamine derivatives [50,67], knows an overwhelming success. This is evidenced by the dozens fluorescent probes, imaging or phototherapy agents bearing an hetero-xanthene dye within their core structure and acting as reporter or photosensitizer, which are published in the literature (both articles and patents) and reviewed in some recent and comprehensive digests [66,68-71]. As the Qian group already observed with symmetrical pyronin Y, replacement (O → $SiMe_2$) on the xanthene framework of unsymmetrical pyronins **2** and **3** produced strong far-red fluorophores **4** and **5** with 100/110 nm and 80/80 nm bathochromic shift respectively of their absorption/emission maxima. Interestingly, the assumed difference in electron-donating ability between *N*-methylindoline

and julolidine moieties (*vide supra*) does not significantly influence the position of absorption/emission bands of such Si-pyronin dyes. The limited effect of aniline *N*-substituents on HOMO-LUMO energy gap of xanthene scaffold seems to be a common trend to silicon-based and related hetero-pyronin dyes [66]. This may be explained by a less effective electronic conjugation between the donating group and π-system, linked to changes in molecular orbitals (*i.e.*, electron density and geometry) induced by atom substitution (O → $SiMe_2$). This hypothesis will deserve further investigation by means of *ab initio* calculations. Compared to yellow-orange emissive pyronin dyes **2** and **3**, fluorescence quantum yields of **4** and **5** are altered but remain satisfactory for the far-red spectral range (27% and 42% for emission centered at 650 nm and 640 nm respectively). Interestingly, the overlaying of absorption and excitation spectra confirms that the introduction of the lipophilic $SiMe_2$ moiety did not favor aggregation of **4** and **5** in aq. solution. In addition to these valuable assets required for applications in complex biological media, the most noticeable result arising from the molecular design strategy based on both heteroatom substitution and desymmetrization through mono *N*-substitution, is undoubtedly the marked stability of Si-pyronin dyes **4** and **5** in an aq. medium over a wide range of pH, compared to parent *N*-unsubstituted Si-pyronin **GD81** (see introduction and Fig. 2). By drawing pH-dependent absorption curves (Fig. 4 and ESI for fitted curves, Fig. S44), we were able to determine the pK value of the corresponding hydration equilibrium between Si-pyronin and Si-xanthydrol forms (pK = 8.3 and 9.8 for **4** and **5** respectively). Furthermore, curves clearly show that the hydrolytic stability of **4** and **5** is optimal at pH < 7 and pH < 8 respectively. These various characterizations have enabled us to identify mono-julolidine-based Si-pyronin dye **5** as an attractive fluorogenic aniline for designing activatable far-red fluorescent probes, that may be regarded as a useful complement to mono-julolidine-based Si-rosamine **HMJSiR** recently reported by the Urano group [72].

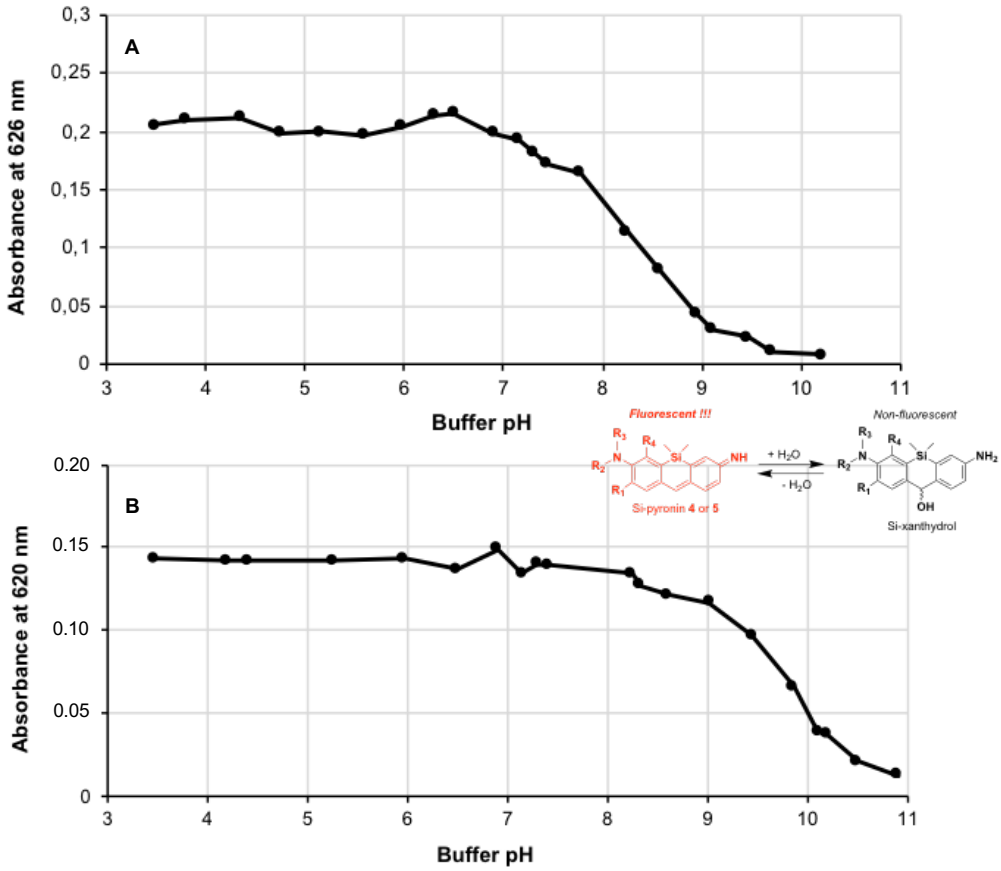

Fig. 4. pH-Dependant maximum absorbance (626 nm or 620 nm) curve for Si-pyronins **4** (A) and **5** (B) (concentration: 5.0 or 3.5 μM in the corresponding buffer, 15 min of incubation before absorbance measurement).

4. Conclusion

In summary, novel analogs of 3-imino-3*H*-xanthen-6-amine (pyronin), the structurally simplest member of the class of xanthene-based fluorophores, bearing an intracyclic silicon atom and/or a single tertiary aniline donor unit were successfully synthesized. First, we devised an original two-step synthetic strategy to readily achieve structural desymmetrization of pyronin scaffold, based on a copper-catalyzed Ullmann cross-coupling reaction as the key step. As a natural extension of our work, this versatile methodology could also be applied to facile preparation of other xanthene-based fluorophores such as rhodamines, rhodols and rosamines, with the dual aim of providing molecular diversity and fine tuning spectral properties of these photoactive compounds. The synthetic access to silicon analogs of these unsymmetrical pyronin dyes was less straightforward and more laborious because the Hitchcock methodology is always a prerequisite in the preparation of Si-xanthene derivatives. However, the availability of Si-pyronin dyes **4** and **5** has enabled us to perform some photophysical and stability studies in simulated physiological conditions. The latter ones clearly support the relevance of molecular

design strategy based on both heteroatom substitution (O → $SiMe_2$) and molecular desymmetrization of xanthene scaffold through incorporation of a bulky tertiary aniline fragment, to obtain high-performance aniline-based fluorophores. Interestingly, in addition to their use as fluorogenic dyes in "smart" probes based on protection-deprotection of a primary amino group [34-36], these novel (Si-)pyronin derivatives will be very useful as references to validate "covalent-assembly" fluorescent probes based on *in situ* formation of (Si-)pyronin triggered by the analyte to be detected [38-42]. Finally, tunable reactivity of their *meso*-position towards different nucleophiles can be used to design reversible reaction-based fluorescent probes particularly well suited for real-time imaging of redox status changes *in vivo* [73-75].

Acknowledgements

This work is part of the project "Pharmacoimagerie et Agent Theranostiques", supported by the Université de Bourgogne and Conseil Régional de Bourgogne through the Plan d'Actions Régional pour l'Innovation (PARI) and the European Union through the PO FEDER-FSE Bourgogne 2014/2020 programs. GDR CNRS "Agents d'Imagerie Moléculaire" (AIM) 2037 is also thanked for its interest in this research topic. G. D. gratefully acknowledges the Burgundy Franche-Comté region for her Ph. D. grant, Doctoral School Carnot-Pasteur (ED553, University of Burgundy) and Agence Nationale de la Recherche (ANR, AAPG 2018, DetectOP_BChE, ANR-18-CE39-0014), for funding her participation to IC3EM 2020. A further financial support from ANR (AAPG 2018, PRCI LuminoManufacOligo, ANR-18-CE07-0045-01), especially for the post-doc fellowship of K. R., is also greatly acknowledged. COBRA lab (UMR CNRS 6014) and Iris Biotech company are warmly thanked for the generous gift of some chemical reagents used in this work. The authors also thank the "Plateforme d'Analyse Chimique et de Synthèse Moléculaire de l'Université de Bourgogne" (PACSMUB, http://www.wpcm.fr) for access to spectroscopy instrumentation, Dr. Myriam Laly (University of Burgundy, PACSMUB) for the determination of TFA content in samples purified by semi-preparative RP-HPLC, Dr. Valérie Chalansonnet and M. Sylvain Orenga (bioMérieux company, R&D Microbiology) for their interest in this work.

Appendix A. Supplementary data

Supplementary data related to this article can be found online at

References

[1] Wright P, Staff Ub. Xanthene Dyes In: Kirk-Othmer Encyclopedia of Chemical Technology: John Wiley & Sons, Inc; 2014. https://doi.org/10.1002/0471238961.2401142023090708.a01.pub2

[2] Duan Y, Liu M, Sun W, Wang M, Liu S, Li QX. Recent progress on synthesis of fluorescein probes Mini-Rev. Org. Chem. 2009; 6: 35-43. https://doi.org/10.2174/157019309787316111

[3] Kim HN, Lee MH, Kim HJ, Kim JS, Yoon J. A new trend in rhodamine-based chemosensors: application of spirolactam ring-opening to sensing ions Chem. Soc. Rev. 2008; 37: 1465-1472. https://doi.org/10.1039/b802497a

[4] Beija M, Afonso CAM, Martinho JMG. Synthesis and applications of Rhodamine derivatives as fluorescent probes Chem. Soc. Rev. 2009; 38: 2410-2433. https://doi.org/10.1039/b901612k

[5] Chen X, Pradhan T, Wang F, Kim JS, Yoon J. Fluorescent Chemosensors Based on Spiroring-Opening of Xanthenes and Related Derivatives Chem. Rev. 2012; 112: 1910-1956. https://doi.org/10.1021/cr200201z

[6] Zheng H, Zhan X-Q, Bian Q-N, Zhang X-J. Advances in modifying fluorescein and rhodamine fluorophores as fluorescent chemosensors Chem. Commun. 2013; 49: 429-447. https://doi.org/10.1039/c2cc35997a

[7] Fu M, Zhang X, Wang J, Chen H, Gao Y. Progress of Synthesis and Separation of Regioisomerically Pure 5(6)-Substituted Rhodamine Curr. Org. Chem. 2016; 20: 1584-1590. https://doi.org/10.2174/1385272820666160202004127

[8] Zhang R, Yan F, Huang Y, Kong D, Ye Q, Xu J, Chen L. Rhodamine-based ratiometric fluorescent probes based on excitation energy transfer mechanisms: construction and applications in ratiometric sensing RSC Adv. 2016; 6: 50732-50760. https://doi.org/10.1039/C6RA06956H

[9] Poronik YM, Vygranenko KV, Gryko D, Gryko DT. Rhodols - synthesis, photophysical properties and applications as fluorescent probes Chem. Soc. Rev. 2019; 48: 5242-5265. https://doi.org/10.1039/C9CS00166B

[10] Ahn Y-H, Lee J-S, Chang Y-T. Combinatorial Rosamine Library and Application to in Vivo Glutathione Probe J. Am. Chem. Soc. 2007; 129: 4510-4511. https://doi.org/10.1021/ja068230m

[11] Kasten FH. Comparisons of pyronin dyes obtained from various commercial sources. 1. History Stain Technol. 1962; 37: 265-275. https://doi.org/10.3109/10520296209114486

[12] Biehringer J. Pyronines Chem. Ber. 1894; 27: 3299-3305.

[13] Clunas S, Strory JMD, Rickard JE, Horsley D, Harrington CR, Wischik CM. Preparation of 3,6-disubstituted xanthylium salts for treatment of tauopathies, (WisTa Laboratories Ltd., Singapore). WO2010067078.

[14] Lavis LD. Teaching Old Dyes New Tricks: Biological Probes Built from Fluoresceins and Rhodamines Annu. Rev. Biochem. 2017; 86: 825-843. https://doi.org/10.1146/annurev-biochem-061516-044839

[15] Prento P. Staining of macromolecules: possible mechanisms and examples Biotech. Histochem. 2009; 84: 139-158. https://doi.org/10.1080/10520290902908810

[16] Wu L, Burgess K. Fluorescent Amino- and Thiopyronin Dyes Org. Lett. 2008; 10: 1779-1782. https://doi.org/10.1021/ol800526s

[17] Han S, Chen Y. One-pot synthesis of N, N, N, N-tetraethyl-9H-xanthene-3,6-diamine and its conversion to pyronine B Dyes Pigm. 2013; 96: 59-62. https://doi.org/https://doi.org/10.1016/j.dyepig.2012.03.034

[18] Butkevich AN, Sednev MV, Shojaei H, Belov VN, Hell SW. PONy Dyes: direct addition of P(III) nucleophiles to organic fluorophores Org. Lett. 2018; 20: 1261-1264. https://doi.org/10.1021/acs.orglett.8b00270
[19] Bachman JL, Escamilla PR, Boley AJ, Pavlich CI, Anslyn EV. Improved Xanthone Synthesis, Stepwise Chemical Redox Cycling Org. Lett. 2019; 21: 206-209. https://doi.org/10.1021/acs.orglett.8b03661
[20] Liu J, Sun Y-Q, Zhang H, Huo Y, Shi Y, Guo W. Simultaneous fluorescent imaging of Cys/Hcy and GSH from different emission channels Chem. Sci. 2014; 5: 3183-3188. https://doi.org/10.1039/c4sc00838c
[21] Sun Y-Q, Liu J, Zhang H, Huo Y, Lv X, Shi Y, Guo W. A Mitochondria-Targetable Fluorescent Probe for Dual-Channel NO Imaging Assisted by Intracellular Cysteine and Glutathione J. Am. Chem. Soc. 2014; 136: 12520-12523. https://doi.org/10.1021/ja504156a
[22] Kawagoe R, Takashima I, Usui K, Kanegae A, Ozawa Y, Ojida A. Rational Design of a Ratiometric Fluorescent Probe Based on Arene-Metal-Ion Contact for Endogenous Hydrogen Sulfide Detection in Living Cells ChemBioChem 2015; 16: 1608-1615. https://doi.org/10.1002/cbic.201500249
[23] Zhang H, Liu J, Sun Y-Q, Huo Y, Li Y, Liu W, Wu X, Zhu N, Shi Y, Guo W. A mitochondria-targetable fluorescent probe for peroxynitrite: fast response and high selectivity Chem. Commun. 2015; 51: 2721-2724. https://doi.org/10.1039/c4cc09122a
[24] He L, Yang X, Liu Y, Weiying L. Colorimetric and ratiometric fluorescent probe for hydrogen sulfide using a coumarin-pyronine FRET dyad with a large emission shift Anal. Methods 2016; 8: 8022-8027. https://doi.org/10.1039/c6ay02537d
[25] Nie H, Jing J, Tian Y, Yang W, Zhang R, Zhang X. Reversible and Dynamic Fluorescence Imaging of Cellular Redox Self-Regulation Using Fast-Responsive Near-Infrared Ge-Pyronines ACS Appl. Mater. Interfaces 2016; 8: 8991-8997. https://doi.org/10.1021/acsami.6b01348
[26] Nie H, Qiao L, Yang W, Guo B, Xin F, Jing J, Zhang X. UV-assisted synthesis of long-wavelength Si-pyronine fluorescent dyes for real-time and dynamic imaging of glutathione fluctuation in living cells J. Mater. Chem. B 2016; 4: 4826-4831. https://doi.org/10.1039/c6tb00938g
[27] Kawagoe R, Takashima I, Uchinomiya S, Ojida A. Reversible ratiometric detection of highly reactive hydropersulfides using a FRET-based dual emission fluorescent probe Chem. Sci. 2017; 8: 1134-1140. https://doi.org/10.1039/C6SC03856E
[28] Yang L, Niu J-Y, Sun R, Xu Y-J, Ge J-F. The application of mitochondrial targetable pyronine-pyridinium skeleton in the detection of nitroreductase Sens. Actuators, B 2018; 259: 299-306. https://doi.org/10.1016/j.snb.2017.12.011
[29] Zhang H, Liu J, Hu B, Wang L, Yang Z, Han X, Wang J, Bai W, Guo W. Dual-channel fluorescence diagnosis of cancer cells/tissues assisted by OATP transporters and cysteine/glutathione Chem. Sci. 2018; 9: 3209-3214. https://doi.org/10.1039/c7sc05407f
[30] Kang Y-F, Niu L-Y, Yang Q-Z. Fluorescent probes for detection of biothiols based on "aromatic nucleophilic substitution-rearrangement" mechanism Chin. Chem. Lett. 2019; 30: 1791-1798. https://doi.org/10.1016/j.cclet.2019.08.013
[31] Malek A, Bera K, Biswas S, Perumal G, Das AK, Doble M, Thomas T, Prasad E. Development of a Next-Generation Fluorescent Turn-On Sensor to Simultaneously Detect and Detoxify Mercury in Living Samples Anal. Chem. 2019; 91: 3533-3538. https://doi.org/10.1021/acs.analchem.8b05268
[32] Ren M, Wang L, Lv X, Liu J, Chen H, Wang J, Guo W. Development of a benzothiazole-functionalized red-emission pyronin dye and its dihydro derivative for imaging lysosomal viscosity and tracking endogenous peroxynitrite J. Mater. Chem. B 2019; 7: 6181-6186. https://doi.org/10.1039/c9tb01525f

[33] Yang M, Fan J, Sun W, Du J, Peng X. Mitochondria-Anchored Colorimetric and Ratiometric Fluorescent Chemosensor for Visualizing Cysteine/Homocysteine in Living Cells and Daphnia magna Model Anal. Chem. 2019; 91: 12531-12537. https://doi.org/10.1021/acs.analchem.9b03386
[34] Chen X, Sun M, Ma H. Progress in spectroscopic probes with cleavable active bonds Curr. Org. Chem. 2006; 10: 477-489. https://doi.org/10.2174/138527206776055312
[35] Grimm JB, Heckman LM, Lavis LD. The chemistry of small-molecule fluorogenic probes Prog. Mol. Biol. Transl. Sci. 2013; 113: 1-34. https://doi.org/10.1016/b978-0-12-386932-6.00001-6
[36] Tang Y, Lee D, Wang J, Li G, Yu J, Lin W, Yoon J. Development of fluorescent probes based on protection-deprotection of the key functional groups for biological imaging Chem. Soc. Rev. 2015; 44: 5003-5015. https://doi.org/10.1039/c5cs00103j
[37] He T, He H, Luo X, Yang Y, Yang Y. Small molecular fluorescent probes based on covalent assembly Sci. Sinica Chim. 2017; 47: 945-954. https://doi.org/doi:https://doi.org/10.1360/N032017-00047
[38] Lei Z, Yang Y. A Concise Colorimetric and Fluorimetric Probe for Sarin Related Threats Designed via the "Covalent-Assembly" Approach J. Am. Chem. Soc. 2014; 136: 6594-6597. https://doi.org/10.1021/ja502945q
[39] Song L, Lei Z, Zhang B, Xu Z, Li Z, Yang Y. A zero-background fluorescent probe for Hg2+ designed via the "covalent-assembly" principle Anal. Methods 2014; 6: 7597-7600. https://doi.org/10.1039/C4AY01729C
[40] Debieu S, Romieu A. In situ formation of pyronin dyes for fluorescence protease sensing Org. Biomol. Chem. 2017; 15: 2575-2584. https://doi.org/10.1039/C7OB00370F
[41] Debieu S, Romieu A. Kinetics improvement of protease-mediated formation of pyronin dyes Tetrahedron Lett. 2018; 59: 1940-1944. https://doi.org/10.1016/j.tetlet.2018.04.010
[42] Renault K, Debieu S, Richard J-A, Romieu A. Deeper insight into the protease-sensitive "covalent-assembly" fluorescent probes for practical biosensing applications Org. Biomol. Chem. 2019; 17: 8918-8932. https://doi.org/10.26434/chemrxiv.9445202.v1
[43] Müller W. Preparation of the 3,6-diaminoxanthylium cation Justus Liebigs Annalen der Chemie 1974: 334-335. https://doi.org/10.1002/jlac.197419740218
[44] Ren T-B, Xu W, Zhang W, Zhang X-X, Wang Z-Y, Xiang Z, Yuan L, Zhang X-B. A General Method To Increase Stokes Shift by Introducing Alternating Vibronic Structures J. Am. Chem. Soc. 2018; 140: 7716-7722. https://doi.org/10.1021/jacs.8b04404
[45] Drexhage K-H, Arden-Jacob J, Frantzeskos J, Zilles A. Carbopyronine fluorescent dyes, their production and their use as markers for biological compounds, (Germany). WO2000064986.
[46] Arden-Jacob J, Frantzeskos J, Kemnitzer NU, Zilles A, Drexhage KH. New fluorescent markers for the red region Spectrochim. Acta, Part A 2001; 57A: 2271-2283. https://doi.org/10.1016/s1386-1425(01)00476-0
[47] Gu L, Yang B, Liu F, Bai Y. Efficient synthetic route to carbopyronine fluorescent dye intermediate Chin. J. Chem. 2009; 27: 1199-1201. https://doi.org/10.1002/cjoc.200990202
[48] Fu M, Xiao Y, Qian X, Zhao D, Xu Y. A design concept of long-wavelength fluorescent analogs of rhodamine dyes: replacement of oxygen with silicon atom Chem. Commun. 2008: 1780-1782. https://doi.org/10.1039/B718544H
[49] Romieu A, Dejouy G, Valverde IE. Quest for novel fluorogenic xanthene dyes: Synthesis, spectral properties and stability of 3-imino-3H-xanthen-6-amine (pyronin) and its silicon analog Tetrahedron Lett. 2018; 59: 4574-4581. https://doi.org/10.1016/j.tetlet.2018.11.031

[50] Koide Y, Urano Y, Hanaoka K, Terai T, Nagano T. Evolution of Group 14 Rhodamines as Platforms for Near-Infrared Fluorescence Probes Utilizing Photoinduced Electron Transfer ACS Chem. Biol. 2011; 6: 600-608. https://doi.org/10.1021/cb1002416
[51] Zhai D, Xu W, Zhang L, Chang Y-T. The role of "disaggregation" in optical probe development Chem. Soc. Rev. 2014; 43: 2402-2411. https://doi.org/10.1039/C3CS60368G
[52] Lin H-S, Paquette LA. A convenient method for determining the concentration of Grignard reagents Synth. Commun. 1994; 24: 2503-2506. https://doi.org/10.1080/00397919408010560
[53] Lin C-K, Wang Y-F, Cheng Y-C, Yang J-S. Multisite Constrained Model of trans-4-(N,N-Dimethylamino)-4'-nitrostilbene for Structural Elucidation of Radiative and Nonradiative Excited States J. Phys. Chem. A 2013; 117: 3158-3164. https://doi.org/10.1021/jp310770s
[54] Adusumalli SR, Rawale DG, Singh U, Tripathi P, Paul R, Kalra N, Mishra RK, Shukla S, Rai V. Single-Site Labeling of Native Proteins Enabled by a Chemoselective and Site-Selective Chemical Technology J. Am. Chem. Soc. 2018; 140: 15114-15123. https://doi.org/10.1021/jacs.8b10490
[55] Viswanadham B, Mahomed AS, Friedrich HB, Singh S. Efficient and expeditious chemoselective BOC protection of amines in catalyst and solvent-free media Res. Chem. Intermed. 2017; 43: 1355-1363. https://doi.org/10.1007/s11164-016-2702-9
[56] Fulmer GR, Miller AJM, Sherden NH, Gottlieb HE, Nudelman A, Stoltz BM, Bercaw JE, Goldberg KI. NMR Chemical Shifts of Trace Impurities: Common Laboratory Solvents, Organics, and Gases in Deuterated Solvents Relevant to the Organometallic Chemist Organometallics 2010; 29: 2176-2179. https://doi.org/10.1021/om100106e
[57] Brouwer AM. Standards for photoluminescence quantum yield measurements in solution Pure Appl. Chem. 2011; 83: 2213-2228. https://doi.org/10.1351/PAC-REP-10-09-31
[58] Anzalone AV, Wang TY, Chen Z, Cornish VW. A Common Diaryl Ether Intermediate for the Gram-Scale Synthesis of Oxazine and Xanthene Fluorophores Angew. Chem., Int. Ed. 2013; 52: 650-654. https://doi.org/10.1002/anie.201205369
[59] Varejão JOS, Varejão EVV, Fernandes SA. Synthesis and Derivatization of Julolidine: A Powerful Heterocyclic Structure Eur. J. Org. Chem. 2019; 2019: 4273-4310. https://doi.org/10.1002/ejoc.201900398
[60] Hitchcock CHS, Mann FG, Vanterpool A. 913. The preparation and properties of 10 : 10-disubstituted phenoxsilanes J. Chem. Soc. 1957: 4537-4546. https://doi.org/10.1039/JR9570004537
[61] Durandetti M, Boddaet T. Formation de liaisons Si-C pour la synthèse d'hétérocycles silylés L'Actualité Chimique 2018; 434: 11-17.
[62] Koide Y, Urano Y, Hanaoka K, Piao W, Kusakabe M, Saito N, Terai T, Okabe T, Nagano T. Development of NIR Fluorescent Dyes Based on Si–rhodamine for in Vivo Imaging J. Am. Chem. Soc. 2012; 134: 5029-5031. https://doi.org/10.1021/ja210375e
[63] Lei Z, Li X, Luo X, He H, Zheng J, Qian X, Yang Y. Bright, Stable, and Biocompatible Organic Fluorophores Absorbing/Emitting in the Deep Near-Infrared Spectral Region Angew. Chem., Int. Ed. 2017; 56: 2979-2983. https://doi.org/10.1002/anie.201612301
[64] Hanaoka K, Kagami Y, Piao W, Myochin T, Numasawa K, Kuriki Y, Ikeno T, Ueno T, Komatsu T, Terai T, Nagano T, Urano Y. Synthesis of unsymmetrical Si-rhodamine fluorophores and application to a far-red to near-infrared fluorescence probe for hypoxia Chem. Commun. 2018; 54: 6939-6942. https://doi.org/10.1039/c8cc02451k
[65] Dejouy G, Laly M, Valverde IE, Romieu A. Synthesis, stability and spectral behavior of fluorogenic sulfone-pyronin and sulfone-rosamine dyes Dyes Pigm. 2018; 159: 262-274.
[66] Wang L, Du W, Hu Z, Uvdal K, Li L, Huang W. Hybrid Rhodamine Fluorophores in the Visible/NIR Region for Biological Imaging Angew. Chem., Int. Ed. 2019; 58: 14026-14043. https://doi.org/10.1002/anie.201901061

[67] Egawa T, Koide Y, Hanaoka K, Komatsu T, Terai T, Nagano T. Development of a fluorescein analogue, TokyoMagenta, as a novel scaffold for fluorescence probes in red region Chem. Commun. 2011; 47: 4162-4164. https://doi.org/10.1039/c1cc00078k
[68] Kushida Y, Nagano T, Hanaoka K. Silicon-substituted xanthene dyes and their applications in bioimaging Analyst 2015; 140: 685-695. https://doi.org/10.1039/C4AN01172D
[69] Ikeno T, Nagano T, Hanaoka K. Silicon-substituted Xanthene Dyes and Their Unique Photophysical Properties for Fluorescent Probes Chem. - Asian J. 2017; 12: 1435-1446. https://doi.org/10.1002/asia.201700385
[70] Deng F, Xu Z. Heteroatom-substituted rhodamine dyes: Structure and spectroscopic properties Chinese Chem. Lett. 2019; 30: 1667-1681. https://doi.org/https://doi.org/10.1016/j.cclet.2018.12.012
[71] Li M, Li Y, Wang X, Cui X, Wang T. Synthesis and application of near-infrared substituted rhodamines Chinese Chem. Lett. 2019; 30: 1682-1688. https://doi.org/https://doi.org/10.1016/j.cclet.2019.06.036
[72] Iwatate RJ, Kamiya M, Umezawa K, Kashima H, Nakadate M, Kojima R, Urano Y. Silicon Rhodamine-Based Near-Infrared Fluorescent Probe for γ-Glutamyltransferase Bioconjugate Chem. 2018; 29: 241-244. https://doi.org/10.1021/acs.bioconjchem.7b00776
[73] Chu T-s, Lu R, Liu B-t. Reversibly monitoring oxidation and reduction events in living biological systems: Recent development of redox-responsive reversible NIR biosensors and their applications in in vitro/in vivo fluorescence imaging Biosens. Bioelectron. 2016; 86: 643-655. https://doi.org/10.1016/j.bios.2016.07.039
[74] Kaur A, Kolanowski JL, New EJ. Reversible Fluorescent Probes for Biological Redox States Angew. Chem., Int. Ed. 2016; 55: 1602-1613. https://doi.org/10.1002/anie.201506353
[75] Li B, He Z, Zhou H, Zhang H, Cheng T. Reversible fluorescent probes for chemical and biological redox process Chin. Chem. Lett. 2017; 28: 1929-1934. https://doi.org/10.1016/j.cclet.2017.08.055